



## 1 Particle Swarm Optimization for Surface complexation with the 2 PHREEQC geochemical model

---

3 Ramadan Abdelaziz<sup>1,2</sup>, Broder J. Merkel<sup>2</sup>, Mauricio Zambrano-Bigiarini<sup>3</sup>, Sreejesh Nair<sup>4</sup>

4 <sup>1</sup> College Of Engineering, A'Sharqiyah University

5 <sup>2</sup> TU Bergakademie Freiberg, Germany

6 <sup>3</sup> Department of Civil Engineering, Universidad de La Frontera, Chile

7 <sup>4</sup> Institute of Environmental Physics, University of Bremen, Germany

8 Email: [ramawaad@gmail.com](mailto:ramawaad@gmail.com), [ramadan.abdelaziz@asu.edu.om](mailto:ramadan.abdelaziz@asu.edu.om)

### 9 Abstract

10 Recently, Particle Swarm Optimization (PSO) techniques have attracted many researchers to optimize  
11 model parameters in several fields of research. This paper explains, for the first time, how to interface the  
12 hydroPSO R optimization package with the PHREEQC geochemical model, version 2.3.1. Sorption of  
13 metals on minerals is a key process in treatment water, natural aquatic environments, and other water  
14 related technologies. Sorption processes can be simulated by means of surface complexation models.  
15 However, determining thermodynamic constants for surface species from batch experiments requires a  
16 robust parameter estimation tool that does not get stuck in local minima. In this work, uranium at low  
17 concentrations was sorbed on quartz at different pH. Results show that hydroPSO delivers more reliable  
18 thermodynamic parameter values than PEST when both are coupled to PHREEQC using the same  
19 thermodynamic input data (Nair et al., 2014). Post-processing tools included in hydroPSO are helpful for  
20 the interpretation of the results. Thus, hydroPSO is a recommended optimization tool for PHREEQC with  
21 respect to inverse modeling to determine reliable and meaningful thermodynamic parameter values.

22 Keywords: particle swam optimization; hydroPSO; PHREEQC; surface complexation; uranium; sorption

### 23 Introduction and Scope

24 Particle Swarm Optimization technique (PSO) is an evolutionary optimization approach proposed by  
25 Eberhart and Kennedy (1995) and was influenced by the activities of flocks of birds in search of corn  
26 (Kennedy and Eberhart 1995, and Eberhart and Kennedy 1995). Both PSO and genetic algorithms (GA)  
27 shares a few similarities (Eberhart and Shi 1998). GA has evolutionary operators like crossover or



28 selection while PSO does not have it (Eberhart and Shi 1998). Recently, PSO has been implemented in a  
29 wide range of applications, e.g. in the water resources (Zambrano-Bigiarini and Rojas, 2013, Abdelaziz  
30 and Zambrano-Bigiarini 2014), geothermal resources (Ma et al., 2013; Beck et al., 2010), finance and  
31 economics (Das, 2012), in structural design (Kaveh and Talatahari, 2009; Schutte and Groenwold, 2003),  
32 economics and finance (Huang et al., 2006; Das 2012), and applications of video and image analysis  
33 (Donelli and Massa, 2005; Huang and Mohan, 2007). For example, the groundwater model  
34 MODFLOW2000/2005 was linked with PSO to estimate permeability coefficients (Sedki and Ouazar,  
35 2010) and a multi-objective PSO code was used to derive a rainfall runoff model parameters (Gill et al.,  
36 2006). Notwithstanding PSO recent popularity, the PSO has never been used to calculate the parameters of  
37 a surface complexation model (SCMs) simulating sorption behavior of metal and metalloids on mineral  
38 surfaces. Hence, this paper attempts to examine the efficiency and effectiveness of PSO for parameter  
39 estimation of a surface complexation model as is PHREEQC (Parkhurst and Appelo, 1999).

40 Nowadays, a number of PSO software codes exist such as MADS (Harp and Vesselinov, 2011; Vesselinov  
41 and Harp, 2012) and OSTRICH (Matott, 2005), with most of the codes using the basic PSO formulation  
42 developed in 1995. However, in this paper we use the latest Standard Particle Swarm Optimization  
43 proposed in literature (Clerk, 2012; Zambrano-Bigiarini et al., 2013), named SPSO2011, as implemented  
44 in the *hydroPSO* R package (R Core team, 2016) version 0.3-3 (Zambrano-Bigiarini and Rojas, 2013;  
45 2014). *hydroPSO* is an independent R package that includes the newest Standard PSO (SPSO-2011),  
46 which was specifically developed to calibrate a wide range of environmental models. In addition, the  
47 plotting functions in *hydroPSO* are user-friendly and aid the numeric and visual interpretation of the  
48 optimization results. The source code, installation files, tutorial (vignette), and manual available on  
49 <http://cran.r-project.org/web/packages/hydroPSO>.

50 *hydroPSO* is used in this paper, for the first time, to estimate the parameters of a surface complexation for  
51 U(VI)-Quartz system, to properly capture the non-linear interactions between the model parameters. The  
52 aim of this article is to examine the versatility of *hydroPSO* as parameter estimation tool for geochemical  
53 modeling with PHREEQC -3.1.2.



## 54 **Model description**

55 PHREEQC version 2.3 (Parkhurst and Appelo, 1999) is used to model the sorption by and the database of  
56 Nuclear Energy Agency thermodynamic NEA\_2007 (Grenthe et al., 2007), as well as the LLNL database  
57 (Lawrence Livermore National Laboratory) is used to model sorption. Both databases were modified by  
58 set constant values for  $\text{MUO}_2(\text{CO}_3)_3^{2-}$  and  $\text{M}_2\text{UO}_2(\text{CO}_3)_3^0$  species (M equals Ca, Mg, Sr) taken from  
59 Geipel et al.(2008) and Dong and Brooks (2006, 2008). PHREEQC is a geochemical model code which is  
60 capable to simulate sorption, surface complexation, and other types of reactions. SCMs are considered to  
61 be suitable tools to describe the processes at liquid-solid interfaces (Huber and Lützenkirchen, 2009).  
62 Surface Complexation Modelling (SCM) has been widely employed to simulate the metals sorption from  
63 aqueous solution depending on solution concentration and pH value as well as ionic strength and redox  
64 conditions (Davis et al., 2004; Štamberg et al., 2003; Zheng et al., 2003). It is result of a group of reactions  
65 within the aqueous species in the surface of the sorbent and the bulk solution, which leads to the surface  
66 complexes formation. The constants of surface/sorption reaction (log K) values are inevitable for SCM.  
67 Such constants are universal constants, not site-specific, and hence transferable.

68 There are different SCMs like generalized two layer model (GTLM), nonelectrostatic model (NEM),  
69 constant capacitance model (CCM), diffuse-layer model (DLM), modified triple-layer model (modified  
70 TLM). Here, a generalized two layer model (GTLM) (Dzombak and Morel, 1990) was used to simulate  
71 the sorption behavior of U(VI) on quartz. The GTLM was used instead of other models because it is  
72 relatively simple and can be used in a wide range of chemical conditions. A comprehensive review of  
73 GTLM is presented in Dzombak and Morel (1990). Quartz is a nonporous mineral and non-layered, and  
74 therefore, the actual area of surface is supposed to be equal to the specific surface area. In this study, the  
75 surface of quartz is considered as a single binding site and takes the charge for every surface reaction. The  
76 sorption reactions and log K values are related to the aqueous species and thus depend on the  
77 thermodynamic database used. Uranyl carbonate complexes— $(\text{UO}_2)_2\text{CO}_3(\text{OH})_3^-$ ,  $\text{UO}_2(\text{CO}_3)_2^{2-}$  and  
78  $\text{UO}_2(\text{CO}_3)_3^{4-}$ —are the dominant species under our experimental conditions. Therefore, the surface-  
79 complexation reactions for quartz were calculated with respect to this species.



80 The sorption of U(VI) on quartz were investigated and discussed by (Huber and Lützenkirchen 2009).  
 81 However, formation of Mg-, Ca-, and Sr–Uranyl-Carbonato complexes show a significant impact on  
 82 sorption of uranium on quartz. This was studied by Nair and Merkel (2011) in batch experiments adding  
 83 10 g of powdered quartz to 0.1 liter of water containing rather low U concentrations ( $0.1269 \times 10^{-6}$  M) in  
 84 the absence and existence of Mg, Sr, and Ca (1 mM) at a pH value between 9 and 6.5 in steps of 0.5.  
 85  $\text{NaHCO}_3$  ( $1 \times 10^{-3}$  M) and  $\text{NaCl}$  ( $1.5 \times 10^{-3}$  M) were used as ionic-strength buffers. The low U-  
 86 concentrations were used to avoid precipitation of Ca-U-carbonates. In the non-existence of alkaline earth  
 87 elements, the percentage of uranium was sorbed on quartz ca. 90% independent from pH. In the existence  
 88 of Mg, Sr, and Ca, the percentage of sorption of uranium on quartz declined to 50, 30, and 10%,  
 89 correspondingly (Nair and Merkel, 2011).  
 90 However, Table 1 displays the parameter ranges used to optimize the 6 parameters selected to calibrate  
 91 PHREEQC, based on Nair et al., 2014.

92 **Table 1: Parameters to be calculate through parameter estimation.**

| Name of Parameter                                                                                                                                    | ID | Parameter Range values |     | Calibrated Parameter log K |
|------------------------------------------------------------------------------------------------------------------------------------------------------|----|------------------------|-----|----------------------------|
|                                                                                                                                                      |    | Min                    | Max |                            |
| $\text{Q\_xOH} + \text{UO}_2(\text{CO}_3)_3^{4-} + \text{OH}^- \rightleftharpoons \text{Q\_xOUO}_2(\text{CO}_3)_3^{5-} + \text{H}_2\text{O}$         | K1 | 24                     | 26  | 25.156                     |
| $\text{Q\_xOH} + \text{UO}_2(\text{CO}_3)_2^{2-} + \text{OH}^- \rightleftharpoons \text{Q\_xOUO}_2(\text{CO}_3)_2^{3-} + \text{H}_2\text{O}$         | K2 | 20                     | 23  | 21.18                      |
| $\text{Q\_xOH} + \text{UO}_2\text{CO}_3 \rightleftharpoons \text{Q\_xOUO}_2\text{CO}_3^- + \text{H}^+$                                               | K3 | -8                     | -5  | -5.589                     |
| $\text{Q\_xOH} + \text{UO}_2\text{OH}^+ \rightleftharpoons \text{Q\_xOUO}_2\text{OH} + \text{H}^+$                                                   | K4 | 2                      | 4   | 3.229                      |
| $\text{Q\_xOH} + (\text{UO}_2)_2\text{CO}_3(\text{OH})_3^- \rightleftharpoons \text{Q\_xO}(\text{UO}_2)_2\text{CO}_3(\text{OH})_3^{2-} + \text{H}^+$ | K5 | 5                      | 8   | 6.733                      |



|                                    |    |    |    |        |
|------------------------------------|----|----|----|--------|
| $Q\_xOH + Na^+ \rightleftharpoons$ | K6 | -7 | -4 | -5.842 |
| $Q\_xONa + H^+$                    |    |    |    |        |

Q\_xOH: Silanol surface site

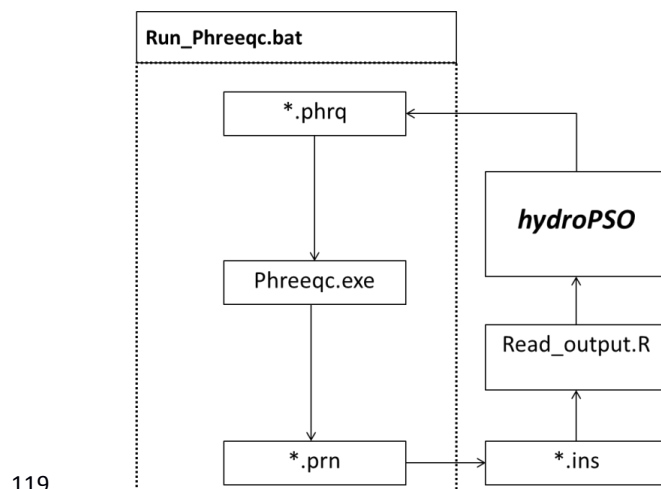
93

94 **Computational implementation**

95 Inverse modeling is a sophisticated issue for modelers as a result of the numerous uncertainties in model  
 96 parameters and observations (e.g., Carrera et al., 2005, Beven, 2006). The *hydroPSO* R package v0.3-3  
 97 (Rojas and Zambrano-Bigiarini, 2012; Zambrano-Bigiarini and Rojas, 2013; 2014) is a model-independent  
 98 optimization package, which has been successfully applied as calibration tool for both hydrogeological  
 99 and hydrological models, requiring no instruction or template files as UCODE (Poeter et al., 2005,  
 100 Abdelaziz and Merkel, 2015) and PEST (Doherty, 2005; 2013) do. In order to couple *hydroPSO* with the  
 101 PHREEQC geochemical model, three text files have to be prepared by the user to handle data transfer  
 102 between the model code and the optimization engine: (i) '*ParamFiles.txt*', which describes the names of a  
 103 set of parameters to be estimated and locations in the model input files to be utilized in the inverse  
 104 procedure, (ii) '*ParamRanges.txt*', which defines the minimum and maximum values that each selected  
 105 parameter might have during the optimization, and (iii) '*PSO\_OBS.txt*', which contains the observations  
 106 that will be compared against its simulated counterparts. In addition, a user-defined R script file  
 107 ('*Read\_output.R*') have to be prepared, containing the instructions to read model outputs, while an R script  
 108 template provided by *hydroPSO* (Rojas and Zambrano-Bigiarini, 2012) has to be slightly modified by the  
 109 user in order to carry out the optimization. In contrast to coupling PEST with PHREEQC was required to  
 110 run PEST with PHREEQC. PEST needs ASCII output and input files. The four files were required: i)  
 111 template files (\*.tpl), ii) instruction files (\*.ins), iii) a main control file (\*.pst), and iv) a batch file to  
 112 execute PHREEQC and PEST(\*.bat) . Template files were built to modify the input files for PHREEQC  
 113 with other values while an instruction file was employed to extract the simulated values from the output  
 114 file for PHREEQC. The main control file includes a model application will be run, the observations,  
 115 parameters to be estimated, control data keywords, and etc. For further information about PEST read the  
 116 manual is recommended. However, Figure 1 shows the key files used to couple PHREEQC with



117 hydroPSO, and explains the flowchart and files involved in the inverse modelling of the surface  
 118 complexation constants for the U(VI) sorption model.



119

120 **Figure 1: Flow chart with files involved in inverse modeling of surface complexation constants for**  
 121 **uranium carbonate (U(VI)) species on quartz with the PHREEQC geochemical model.**

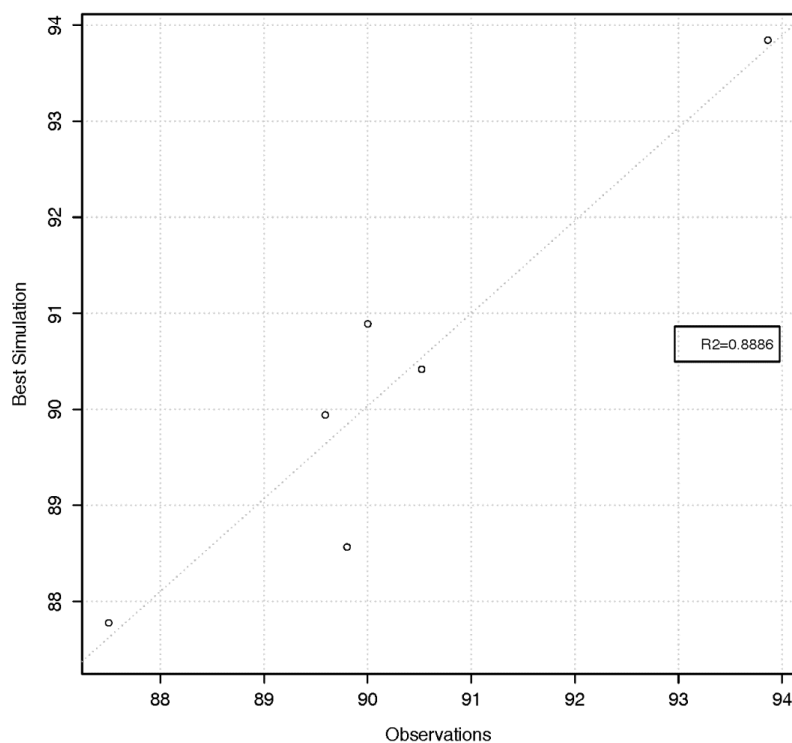
122 For numerical optimization, the residual sum of the squared (*RSS* or *SSR*, see Equation (1)) was utilized to  
 123 compute the goodness of fit (*GoF*) between the corresponding model outputs ( $C^s$ ) and observed values  
 124 ( $C^o$ ) for every time step  $i$ . After some initial trials, the number of maximum iterations  $T$  was set to 200  
 125 and the number of particles used to search for the minimum *RSS* in the parameter space was fixed at 10  
 126 (i.e., 2000 runs of the model). The rest of parameters were set to the default values defined in hydroPSO.  
 127 More information about SPSO 2011 can be found in Clerc (2012), Zambrano-Bigiarini et. al. (2013),  
 128 while detailed information about hydroPSO can be found in Zambrano-Bigiarini and Rojas (2013). Finally,  
 129 all the input files required for running PHREEQC and hydroPSO can be found in the supplementary  
 130 material (<https://doi.org/10.5281/zenodo.803874>), including all the optimization results.

$$SSR = \sum_{i=1}^n (C_i^s - C_i^o)^2 \quad (1)$$



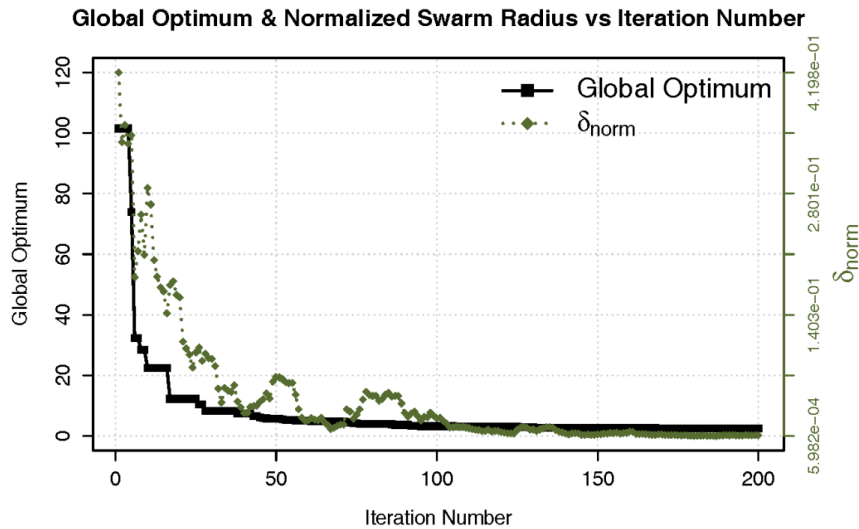
## 131 Results and Discussion

132 One of the vital and useful approaches to evaluate the efficacy of model performance is through  
 133 plotting the simulation against observed values (visualizing outcome of model). The variable observed  
 134 sorption ratio and the calculated sorption ratio were compared in Figure 2. It is clear that there is a very  
 135 good fit between the calculated and the experimentally observed values. The determination coefficient  
 136 ( $r^2$ ), in this case almost 0.8886, is worthwhile and indicates a good match between the observed and  
 137 calculated values (Figure 2). Only 100 iterations were enough to achieve the region of the global  
 138 optimum, i.e.,  $100 \times 10 = 1000$  model runs. The rest iterations numbers were placed to refine the search as  
 139 shown in Figure 3.



140

141 **Figure 2: Scatter plot with the experimentally observed and calculated values of uranium carbonate**  
 142 **(sorption %).**



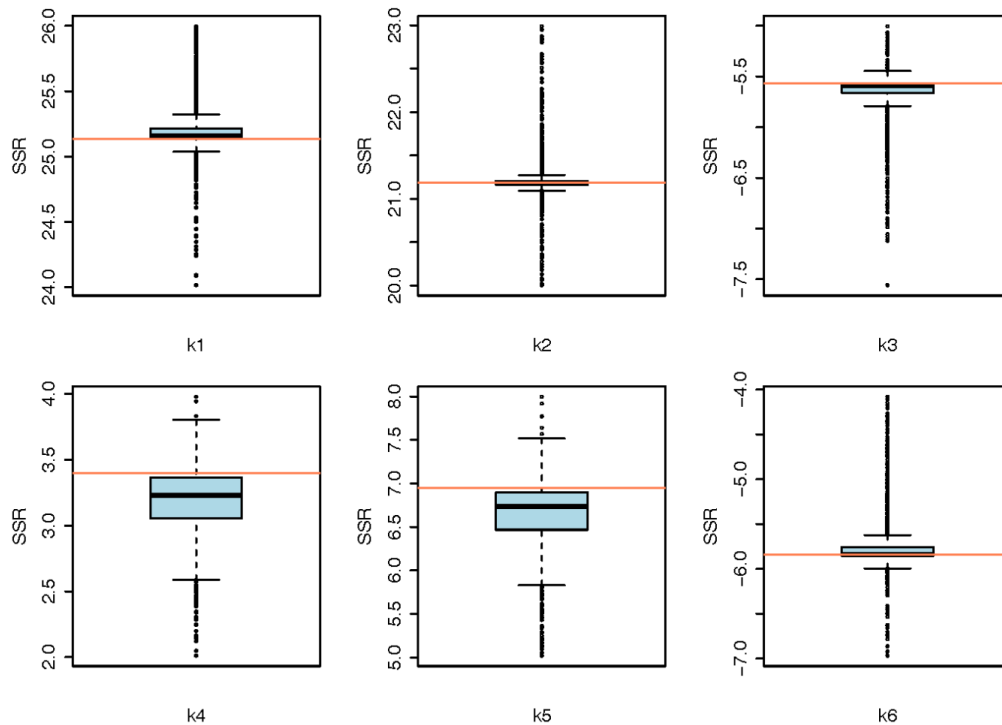
143

144 **Figure 3: Evolution of the normalized swarm radius ( $\delta_{norm}$ ) and the global optimum (SSR) over**  
145 **200 iterations.**

146 However, Figure 3 shows the evolution of the global optimum (best model performance for a given  
147 iteration, i.e., smallest SSR) and the normalized swarm radius ( $\delta_{norm}$ , a measure of the spread of the  
148 population flying over the range of search-space) versus the iterations number. One may observe that both  
149  $\delta_{norm}$  and the global optimum become smaller with an increasing iteration number, which indicates that the  
150 main particles are “flying” around a small portion of the solution space. The optimum value was achieved  
151 when the SSR was ca. 2.52.

152 Boxplots in Figure 4 are valuable graphical representation of the values sampled during optimization.  
153 The bottom and top of the box demonstrate the first and third quartiles, respectively. The horizontal line  
154 within the box stands for the median. Finally, points outside the notches are considered to be outliers,  
155 where notches are within  $\pm 1.58IQR/\sqrt{n}$ , while IQR represents the interquartile range and  $n$  the  
156 number of points. The horizontal red lines in Figure 4 point out the optimum value found during  
157 optimization for each parameter.



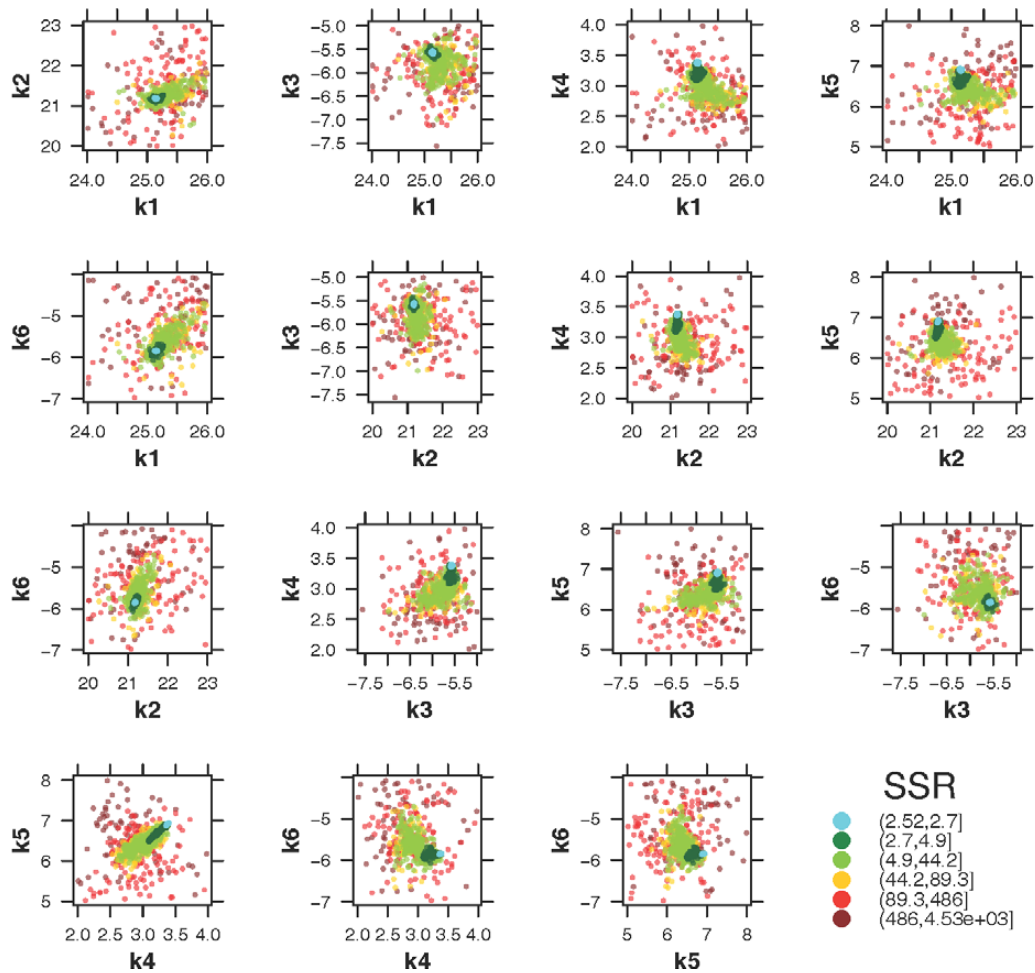


158

159 **Figure 4: Boxplots showing for calibrated parameter. The horizontal red lines indicate the optimum**  
160 **value for each parameter.**

161 The SSR was chosen as an indicator for goodness of fit (*GoF*). Two dimensional dotted plots in Figure  
162 5 depict the goodness of fit achieved by different parameter sets. They are suitable for identifying  
163 parameter ranges, leading to high or roughly the same model performance (equifinality, Beven and  
164 Binley, 1992). Parameter names are defined in Table 1.

165 Figure 5 shows the model performance as function of the interaction of different parameter ranges.  
166 The (quasi) three-dimensional dotted plot shown in Figure 5 is a projection of the values of pairs of  
167 parameters onto the model response surface (goodness-of-fit value). Parameter values where the model  
168 presents high performance are shown in light-blue (high points density), whilst the parameter values  
169 where the model shows low performance are shown in dark-red (low points density). This figure was  
170 used to identify regions of the solution space with good and bad model performances (Figure 5).



171

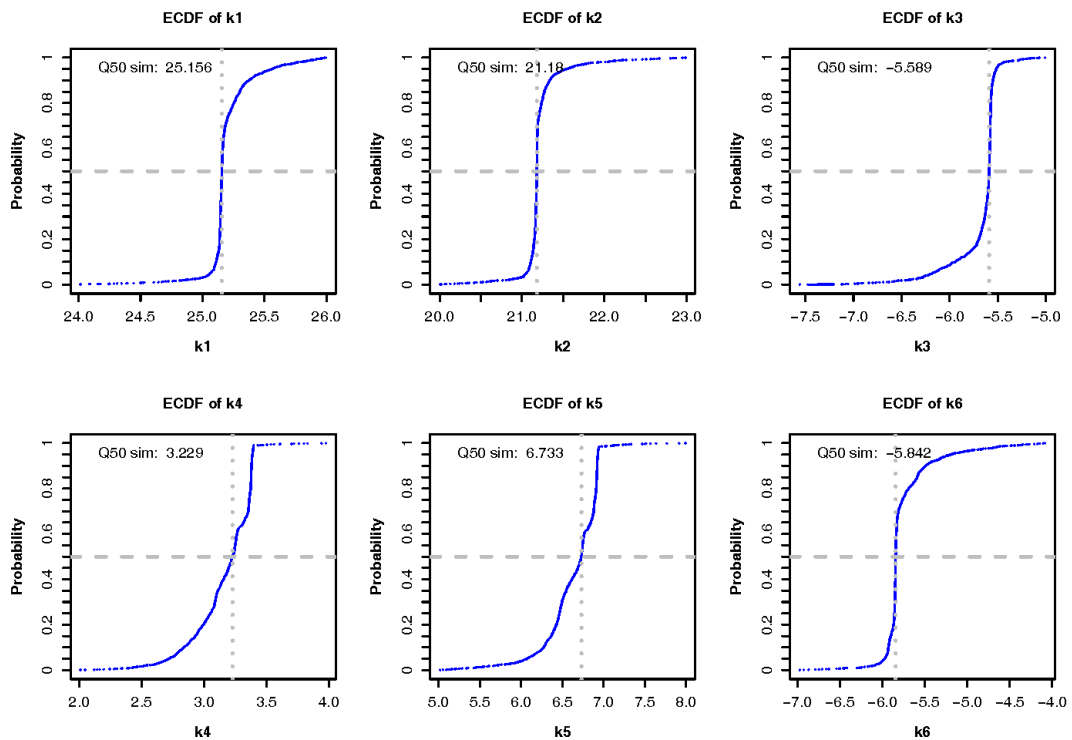
172 **Figure 5: Quasi three-dimensional dotted plots.**

173 Visual inspection of Figure 5 shows a good exploratory capability of PSO because the particles are  
 174 well spread over the entire range space. It is clearly visible that the parameter samples are denser around  
 175 the optimum value (lowest SSR), proving a low standard deviation around the optimum value.  
 176 Nevertheless, the optimum value obtained for K3 and K2 indicated the particles were converging into a  
 177 small region of the solution space.

178 Figure 6 and Figure 7 give a graphical summary for calibrated parameters. Empirical Cumulative  
 179 Density Functions (ECDF) in Figure 6 shows the sampled frequencies for the six parameters. The

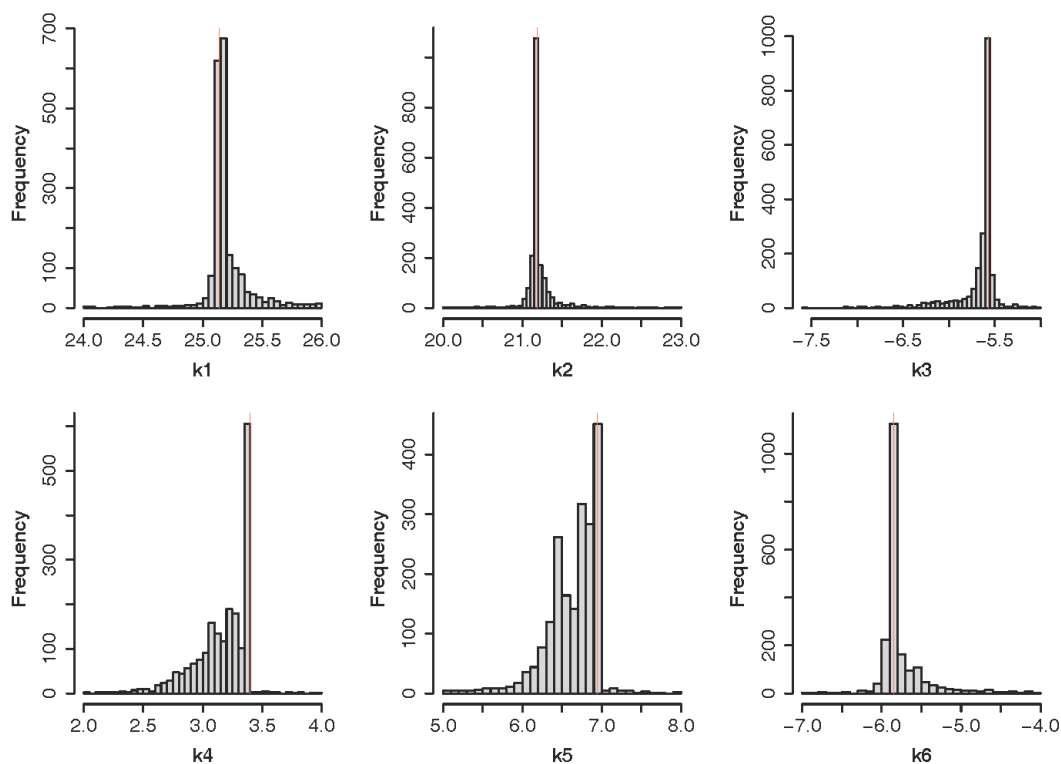


180 horizontal gray dotted lines show a median of the distribution (cumulative probability equal to 0.5) while  
181 the vertical gray dotted lines depict a cumulative probability of 0.5, and its value is displayed in the top of  
182 every figure (Figure 6). The vertical red line point out the optimum value achieved for each parameter  
183 (Figure 7). Both histograms and ECDFs show near-normal distributions for K1 and K2, while k4 and k5  
184 follow a skewed distribution with more sampled values near the upper boundary.



185

186 **Figure 6: Empirical cumulative density functions against each parameter of parameter values.**

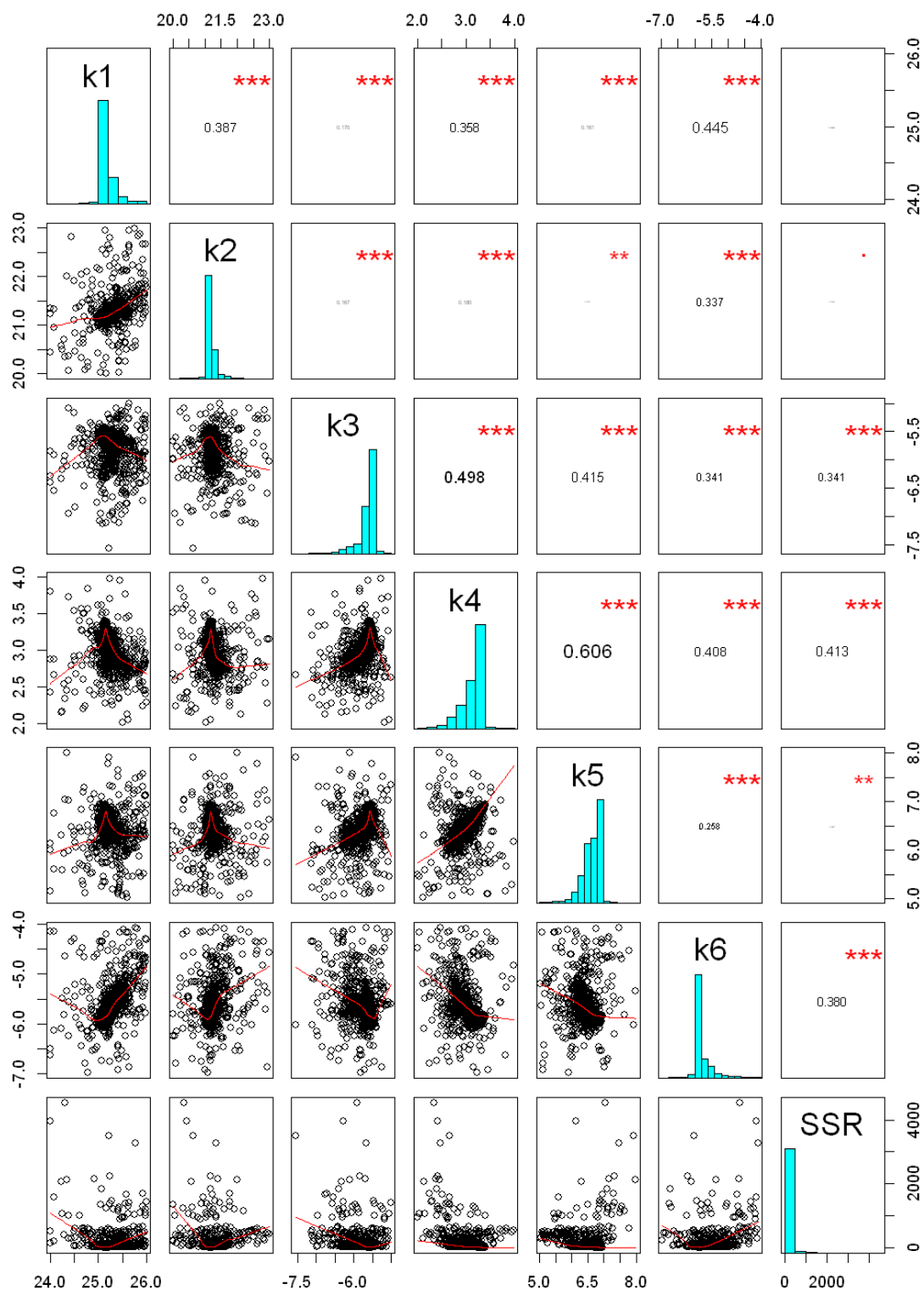


187

188 **Figure 7: Histograms of calibrated parameter values.**

189

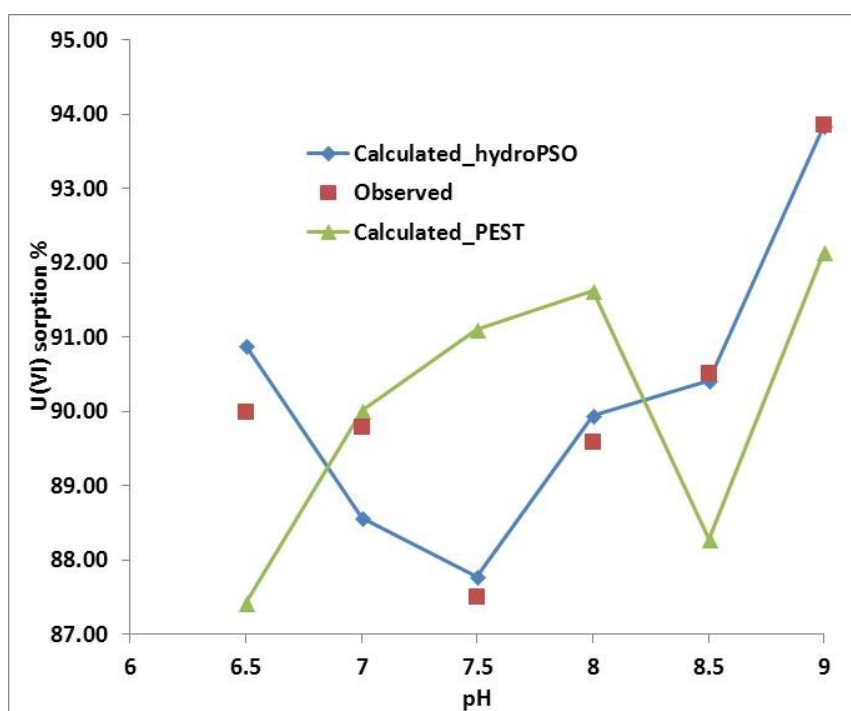
190 **Figure 8** illustrates the correlation matrix among K values and model performance (SSR), with horizontal  
191 and vertical axes displaying the ranges used for the calibration of each parameter. The figure represents  
192 that highest correlation coefficient occurred among the measure of model performance (SSR) and k4, k6,  
193 and k3. In addition, a higher correlation coefficient was observed between k4 and k5, k3 and k4, and k1  
194 and k6.





196 **Figure 8: Correlation matrix among model performance (SSR) and calculated parameters.**  
197 **Vertical and horizontal axes illustrate the physical range utilized for parameter identification. \*\*\***  
198 **stands for a  $p < 0.001$  ; \*\* stands for  $p < 0.01$ , according to level of statistical significance**

199 Figure 9 shows the model output using hydroPSO fitted log-K values and the monitored sorption ratio.



200

201 **Figure 9: Observed and simulated sorption of uranium in quartz vs pH with both PEST and**  
202 **hydroPSO calibrated log-k values.**

203 It is worthwhile to mention that the surface complexation constants for the equations 1, 2, and 4 are  
204 more important and the equations that are less important are 3, 5, and 6 in optimizing the “log K” values.  
205 It proves that  $\text{UO}_2(\text{CO}_3)_3^{4-}$ ,  $\text{UO}_2(\text{CO}_3)_2^{2-}$ , and  $\text{UO}_2\text{OH}^+$  are the most dominate species sorption on quartz.  
206 From the optimized model, the surface complexation constants for the equations 2 and 4 was optimized to  
207 be 21.18 and 3.229 respectively, which is higher than the electrostatic (ES) and nonelectrostatic (NES)  
208 models, while the optimized value for equation 1 is 25.156, which is higher than the NES model and  
209 almost the same as the ES model.



210 Comparing the results of optimized log-K values with hydroPSO with previous work done by Nair et  
211 al. (2014). PEST was applied for the similar case and the same data, we can show that the log k values  
212 obtained with hydroPSO are better than those obtained with PEST. The main reason is that PSO is a  
213 global optimization technique, which searches for optimum values in the whole parameters space, while  
214 PEST searches on a neighborhood of the initial solution. In particular, PEST carries out inverse modelling  
215 by computing value of parameter that minimizes a weighted least-squares objective function via Gauss-  
216 Marquardt-Levenberg non-linear regression method (Marquardt, 1963). Actually, a major drawback of  
217 PEST, as of all gradient-based techniques, is the dependency of the quality of the optimization results  
218 upon the initial point used for the optimization, which might lead to a local optimum rather than the global  
219 one. Thus, PSO techniques offer promising possibilities for similar surface complexation and reactive  
220 transport applications in hydrogeology and hydrochemistry.

## 221 **Conclusions**

222 The coupling of hydroPSO and PHREEQC was successfully done to estimate surface complexation  
223 constants for uranium (VI) species on quartz. The open-source hydroPSO R package was confirmed to be  
224 a robust tool for inverse modeling of surface complexation models with PHREEQC and allowed a prompt  
225 evaluation of the calibration results. Furthermore, thermodynamic values obtained with *hydroPSO*  
226 provided a better match to observation sorption rate in comparison to those obtained with PEST, using the  
227 same input data. This is documented by the higher coefficient of determination for the results based on  
228 *hydroPSO*.

229 Finally, the paper basically treats the coupling of a parameter estimation code with PHREEQC. A  
230 limited data set was used from a paper published by Nair and Merkel (2011) and Nair et al. (2014) to  
231 demonstrate the ability of PSO as an optimizer for a geochemical model as PHREEQC. The examples  
232 were used only for testing the coupled-codes to show the link between PHREEQC and hydroPSO. Indeed,  
233 it is obvious that more comprehensive data sets in the future are needed to get a best-fit and smaller degree  
234 of uncertainty.



235 **Data availability**

236 PHREEQC is available in the following <http://www.hydrochemistry.eu/ph3/index.html>. Source code,  
237 tutorials, and reference manual of hydroPSO can be obtained from [https://CRAN.R-](https://CRAN.R-project.org/package=hydroPSO)  
238 [project.org/package=hydroPSO](https://CRAN.R-project.org/package=hydroPSO). The PHREEQC model input files along with the R scripts used for  
239 coupling it with hydroPSO and the model outputs can be obtained from the Zenodo repository  
240 (<https://zenodo.org/record/803874#.WTigbY26zIV>).

241 **References**

- 242 Abdelaziz, R.; ZAMBRANO-BIGIARINI, M. Particle Swarm Optimization for inverse modeling of solute  
243 transport in fractured gneiss aquifer. *Journal of contaminant hydrology*, **2014**, 164. Jg., S. 285-298.
- 244 Abdelaziz, R.; Merkel, B.J., 2015. Sensitivity analysis of transport modeling in a fractured gneiss aquifer.  
245 *Journal of African Earth Sciences*, 103, pp.121-127.
- 246 Beck, M.; Hecht-Méndez, J.; de Paly, M.; Bayer, P.; Blum, P.; Zell, A. Optimization of the energy  
247 extraction of a shallow geothermal system. 2010 IEEE Congress on Evolutionary Computation (CEC),  
248 **2010**, pp. 1–7.
- 249 Benedikt, G. 797 VA Computrace–voltammetric trace determination of uranium (VI) in drinking and  
250 mineral water. *Metrohm Information*, **2007**, Nr. 2.
- 251 Beven, K. fA manifesto for the equifinality thesis. *Journal of hydrology*, **2006**, 320. Jg., Nr. 1, S. 18-36.
- 252 Beven, K.J.; Binley, A. The future of distributed models — model calibration and uncertainty prediction.  
253 *Hydrol. Process.*, **1992**, 6, 279–298.
- 254 Clerc, M. Standard Particle Swarm Optimisation. Technical Re-port. Particle Swarm Central.  
255 [http://clerc.maurice.free.fr/ps0/SPSO\\_descriptions.pdf](http://clerc.maurice.free.fr/ps0/SPSO_descriptions.pdf). [Online. Last accessed 24-Sep-2012], **2012**.
- 256 Carrera, J; Alcolea, A.; Medina, A.; Hidalgo, J.; Slooten, L. J.. Inverse problem in hydrogeology.  
257 *Hydrogeology journal*, **2005**, 13. Jg., Nr. 1, S. 206-222.
- 258 Das, Parichay. Economics of Distributed Generation Using Particle Swarm Optimization: A Case Study.  
259 *Economics*, **2012**, 1. Jg., Nr. 5.
- 260 Davis, J.A.; Meece, DE, Kohler M, Curtis GP (2004) Approaches to surface complexation modeling of  
261 uranium(VI) adsorption on aquifer sediments. *Geochimica Et Cosmochimica Acta*, **2004**, 68 (18):3621-  
262 364.1.
- 263 Doherty, J. PEST: model-independent parameter estimation, user manual. Technical Report (5th  
264 ed.)Watermark Numerical Computing, Brisbane, Queensl., Australia, **2005**.
- 265 Doherty, J. Addendum to the PEST manual. Technical Report Watermark Numerical Computing, Brisbane,  
266 Queensl., Australia, **2013**.
- 267 Dong, W.M.; Brooks, S.C. Determination of the formation constants of ternary complexes of uranyl and  
268 carbonate with alkaline earth metals ( $Mg^{2+}$ ,  $Ca^{2+}$ ,  $Sr^{2+}$ , and  $Ba^{2+}$ ) using anion exchange method. *Environ*  
269 *Sci Technol*, **2006**, 40:4689–4695.
- 270 Dong, W.M.; Brooks, S.C. Formation of aqueous  $MgUO_2(CO_3)_3^{2-}$  complex and uranium anion exchange  
271 mechanism onto an exchange resin. *Environ Sci Technol*, **2008**, 42:1979–1983.





- 272 Donelli, M., Massa, A. Computational approach based on a particle swarm optimizer for microwave  
273 imaging of two-dimensional dielectric scatterers. *IEEE Transactions on Microwave Theory and*  
274 *Techniques*, **2005**,53(5), 1761-1776.
- 275
- 276 Dzombak, D.A.; Morel, F.M. Surface complexation modeling: Hydrous ferric oxide. John Wiley & Sons,  
277 New York, **1990**.
- 278 Eberhart, R.; Kennedy, J. A new optimizer using particle swarm theory. *Proceedings of the Sixth*  
279 *International Symposium on Micro Machine and Human Science*, 1995. MHS'95, 1995, pp. 39–43.
- 280 Eberhart, R.C.; Shi, Y. Comparison between genetic algorithms and particle swarm optimization, in  
281 *Evolutionary Programming VII*, V. Porto, N. Saravanan, D. Waagen, and A. Eiben, Eds. Springer Berlin /  
282 Heidelberg, **1998**, vol. 1447, pp. 611–616. doi: 10.1007/BFb0040812.
- 283 Geipel, G.; Amayri, S.; Bernhard, G. Mixed complexes of alkaline earth uranyl carbonates: a laser-  
284 induced time-resolved fluorescence spectroscopic study. *Spectrochimica Acta Part A-Mol Biomol*  
285 *Spectrosc*, **2008**, 71:53–58.
- 286 Gill, M. K.; Kaheil, Y. H.; Khalil, A.; McKee, M.; Bastidas, L. Multiobjective particle swarm  
287 optimization for parameter estimation in hydrology. *Water Resources Research*, **2006**,42(7).  
288 doi:10.1029/2005WR004528.
- 289 Grenthe, I.; Fuger, J.; Konings R.; Lemire, R.J.; Muller, A.B.; Wanner, J. *The Chemical Thermodynamics*  
290 *of Uranium*. Elsevier: New York, **2007**.
- 291 Harp, D., Vesselinov, V.V., Recent developments in MADS algorithms: ABAGUS and Squads, EES-16  
292 Seminar Series, LA-UR-11-11957, **2011**.
- 293 Huang, F. Y.; Li, R. J.; Liu, H. X.; Li, R. A modified particle swarm algorithm combined with fuzzy  
294 neural network with application to financial risk early warning. In *Services Computing*, 2006. APSCC'06.  
295 *IEEE Asia-Pacific Conference*, IEEE, **2006**, 168-173.
- 296 Huber, F.; Lutzenkirchen, J., Uranyl Retention on Quartz-New Experimental Data and Blind Prediction  
297 Using an Existing Surface Complexation Model. *Aquatic Geochemistry*, **2009**, 15, (3), 443-456.
- 298 Huang, T., & Mohan, A. S. A microparticle swarm optimizer for the reconstruction of microwave images.  
299 *IEEE Transactions on Antennas and Propagation*, **2007**,55(3), 568-576.
- 300 Kaveh, A., Talatahari, S. A particle swarm ant colony optimization for truss structures with discrete  
301 variables. *Journal of Constructional Steel Research*, **2009**,65(8), 1558-1568.
- 302 Kennedy, J.; Eberhart, R. Particle swarm optimization, in: *neural networks*, 1995. *Proceedings. IEEE*  
303 *International Conference on Neural Networks*, **1995**, pp. 1942–1948.
- 304 Ma, R.J.; Yu, N.Y.; Hu, J.Y. Application of particle swarm optimization algorithm in the heating system  
305 planning problem. *Sci. World J.* 11., **2013**, <http://dx.doi.org/10.1155/2013/718345>.
- 306 Marquardt, D. An algorithm for least-squares estimation of nonlinear parameters. *Journal of the Society*  
307 *for Industrial and Applied Mathematics*, **1963**,11. pp. 431–441.
- 308 Matott, L. *Ostrich: An Optimization Software Tool, Documentation and User's Guide*, Version 1.6.  
309 Department of Civil, Structural and Environmental Engineering, University at Buffalo, Buffalo, NY,  
310 **2005**.
- 311 Nair, S.; Merkel B. J. Impact of Alkaline Earth Metals on Aqueous Speciation of Uranium(VI) and  
312 Sorption on Quartz. *Aquatic Geochemistry*, **2011**,1 17 (3):209-219



- 313 Nair, Sreejesh; Karimzadeh, Lotfollah; Merkel, Broder J. Surface complexation modeling of Uranium  
314 (VI) sorption on quartz in the presence and absence of alkaline earth metals. *Environmental Earth*  
315 *Sciences*, **2014**, 71. Jg., Nr. 4, S. 1737-1745.
- 316
- 317 Parkhurst, D.L.; Appelo, C.A. User's Guide to PHREEQC (version 2). A Computer Program for  
318 Speciation, Batch-Reaction, One-Dimensional Transport, and Inverse Geochemical Calculation. USGS,  
319 Water Resources Investigation Report, **1999**, 99 – 4259.
- 320 Poeter, E.; Hill, M.; Banta, E.; Mehl, S.; Christensen, S. UCODE 2005 and six other computer codes for  
321 universal sensitivity analysis, calibration, and uncertainty evaluation. *US Geological Survey Techniques*  
322 *and Methods*, **2005**, vol. 6-A11.
- 323 Poli, R.; Kennedy, J.; Blackwell, T. Particle swarm optimization: an overview. *Swarm Intell.*, **2007** ,1, 33–  
324 57.
- 325 R Core Team. R: A Language and Environment for Statistical Computing. R Foundation for Statistical  
326 Computing. Vienna, Austria. URL: <http://www.R-project.org/>, **2016**.
- 327 Rojas, R.; Zambrano-Bigiarini, M. Tutorial for interfacing hydroPSO with SWAT-2005 and MODFLOW-  
328 2005. Technical Report. URL: [http://www.rforge.net/hydroPSO/files/hydroPSO\\_vignette.pdf](http://www.rforge.net/hydroPSO/files/hydroPSO_vignette.pdf). [Online.  
329 Last accessed 03-Feb-2014], **2012**.
- 330 Schutte, J.F.; Groenwold, A.A. A study of global optimization using particle swarms. *J. Glob. Optim.*,  
331 **2005**,31, 93–108.
- 332 Schutte, J. F., Groenwold, A. A. Sizing design of truss structures using particle swarms. *Structural and*  
333 *Multidisciplinary Optimization*, **2003**, 25(4), 261-269.
- 334 Sedki, A.; Ouazar, D. Swarm intelligence for groundwater management optimization. *Journal of*  
335 *Hydroinformatics*, **2011**,13(3), 520-532.
- 336 Štamberg, K.; Venkatesan, K. A.; Vasudeva Rao, P. R. Surface complexation modeling of uranyl ion  
337 sorption on mesoporous silica. *Colloids and Surfaces A: Physicochemical and Engineering Aspects*, **2003**,  
338 221. Jg., Nr. 1, S. 149-162
- 339 Vesselinov, V.V.; Harp, D.R. Adaptive hybrid optimization strategy for calibration and parameter  
340 estimation of physical process models. *Computers & Geosciences*, **2012**, 49, 10–20.  
341 doi:10.1016/j.cageo.2012.05.027.
- 342 Zambrano-Bigiarini, M.; Rojas, R. A model-independent Particle Swarm Optimisation software for model  
343 calibration. *Environmental Modelling & Software*, **2013**, 43, 5-25. doi:10.1016/j.envsoft.2013.01.004.
- 344 Zambrano-Bigiarini, M.; Rojas, R. hydroPSO: Particle Swarm Optimisation, with focus on Environmental  
345 Models. URL: <http://www.rforge.net/hydroTSM/>, <http://cran.r-project.org/web/packages/hydroTSM/>. R  
346 package version 0.3-3, **2014**.
- 347 Zambrano-Bigiarini, M., Clerc, M., & Rojas, R. (2013, June). Standard particle swarm optimisation 2011 at cec-  
348 2013: A baseline for future pso improvements. In *Evolutionary Computation (CEC), 2013 IEEE Congress on* (pp.  
349 2337-2344). IEEE.
- 350 Zheng, Z.; Tokunaga, T. K.; Wan, J. Influence of calcium carbonate on U (VI) sorption to soils.  
351 *Environmental science & technology*, **2003**, 37. Jg., Nr. 24, S. 5603-5608.